

Gating of the Squid Sodium Channel at Positive Potentials:

II. Single Channels Reveal Two Open States

Ana M. Correa and Francisco Bezanilla

Department of Physiology, School of Medicine, University of California at Los Angeles, Los Angeles, CA 90024, and
Marine Biological Laboratory, Woods Hole, MA 02543 USA

ABSTRACT Single-channel recordings from squid axon Na^+ channels were made under conditions of reverse sodium gradient. In the range of potentials studied, $+40$ – $+120$ mV, channels opened promptly after depolarization, closed and reopened several times during the pulse. In patches containing only one channel, the distributions of open dwell times showed two components showing the existence of a second open state. The ensemble average of single-channel records showed incomplete inactivation that became more pronounced at more positive potentials, showing that the maintained phase of the current is the result of only one type of sodium channel with two open states. Analysis of bursts indicated that the dwell times of the events at the onset of the depolarization are longer than those later in the pulse. The dwell open times of the first events could be fitted with a single exponential. This indicated that the channels open preferentially through the first open state, the access to the second open state happening subsequently. Maximum likelihood analysis was used to evaluate several possible kinetic schemes incorporating a second open state. The best model to fit the data from single channels, and consistent with the data from macroscopic and gating currents, has a second open state evolving from the inactivated state. A kinetic model is proposed that incorporates information obtained from dialyzed axons.

INTRODUCTION

Since the work by Chandler and Meves (1970a, b) on the properties of the sodium conductance, it has become clear that sodium current inactivation in squid axons is incomplete at positive potentials and under the conditions of inverse sodium gradients. As they proposed, this could arise from either an independent conductance activating at positive potentials or a change in the characteristics of the conductance at those potentials (Chandler and Meves, 1970b, c). An additional issue was the influence that internal ions might have on the process of inactivation. High internal sodium could interfere with the inactivating process to the extent of producing incomplete inactivation, as was first described by Adelman and Senft (1966). The influence of internal cations on sodium channel inactivation has been the subject of study by several groups (Oxford and Yeh, 1985; Goldman, 1988; Keynes et al., 1992a, b; Keynes and Meves, 1993), the main finding being that high concentrations of internal cations do in fact slow down inactivation. Worth mentioning is the role played by organic ions commonly used as sodium substitutes. With tetramethylammonium and tetraethylammonium, in particular, inactivation of sodium currents is slower and less complete.

In the current terminology, two separate sodium conductances would suggest either a different channel population or another conducting state. If it is another channel, this would

activate at positive potentials and contribute to the plateau phase of the current. Conversely, a change in the gating properties of the channel at positive potentials would be evident at the single-channel level. In this case, differences in rate constants, probability of opening, dwell times in closed and open states should account for the macroscopic changes observed.

In this paper we present evidence that a single type of sodium channel with two open states gives rise to the macroscopic characteristics of the sodium conductance of the squid giant axon. The data shows that changes in the kinetics of a single type of sodium channel are responsible for the behavior at positive potentials, consistent with the results of the previous paper. The existence of the plateau phase of sodium currents at positive potentials does not depend on the orientation of the gradient. Several kinetic sequential models are evaluated by maximum likelihood analysis of single-channel data. Incorporating information obtained from macroscopic ionic and gating current experiments (accompanying paper), we propose a model with a second open state, the access to which is enhanced by increasing depolarization. Previous partial reports of this work have been made (Bezanilla and Correa, 1991, 1992).

MATERIALS AND METHODS

Squid axon preparation

All the experiments were done using giant axons of the North Atlantic squid *Loligo pealei* obtained at the Marine Biological Laboratory in Woods Hole, MA. The axons were dissected from the mantle and cleaned of debris and extra connective tissue under regular sea water at 16°C . A piece of axon approximately 1 cm in length was tied at both ends with regular suture floss, cut from the rest, and transferred to the experimental chamber.

Received for publication 10 November 1993 and in final form 15 March 1994.

Address reprint requests to Ana M. Correa, Department of Physiology, UCLA, School of Medicine, 10833 LeConte Avenue, Los Angeles, CA 90024.

© 1994 by the Biophysical Society

0006-3495/94/06/1864/15 \$2.00

Cut-open axon technique

The technique to cut open the axon has been previously described in detail (Llano et al., 1988; Bezanilla and Vandenberg, 1990). In brief, the piece of axon is pinned down onto the Sylgard (Dow-Corning, Midland, MI)-coated surface of the chamber and cut lengthwise with fine dissection scissors with blunted ends. Transverse cuts at both ends aid careful flattening of the axon on the bottom surface using blunt-end tweezers. This is done in artificial sea water (ASW) without potassium (0 K⁺ ASW; for composition see Table 1). The axon is left in the 0 K⁺ ASW for about 3–5 min, rinsed, and changed to an external (bath) solution with no Ca⁺⁺. Until this point the entire procedure is done at room temperature. Once in the bath solution, the chamber is cooled down (4°C, unless otherwise stated) using Peltier units controlled by a feedback mechanism.

Patch clamp recording

In the cut-open axon, the interior surface is exposed, and the patches form naturally in the outside-out configuration (Hamill et al., 1981). Patch pipettes pulled from 7052 glass capillaries (Garner Glass Co., Claremont, CA) coated with Sylgard 184 (Dow-Corning) with tip resistances of 3–15 Mohms were approached to the axonal surface with applied positive pressure. When the resistance of the pipette increased to double, the positive pressure was relieved, and normally seals formed quickly thereafter. On some occasions slight suction was used to aid seal formation. Most of the patch-pipette manipulation was done manually except for the last stretch when a motorized jogging controller was used for the final approach. Once the seal was formed, the pipette was withdrawn slowly to produce patch excision. During recording, the tip of the pipette was kept far from the axonal surface. This made the solution change faster and more efficiently. The convention used for the solutions was the external (bath)/internal (pipette). Data from three patches are presented here. Two of those had a single sodium channel and were analyzed in detail. The single-channel activity in these patches was similar to that observed in other patches with additional channels.

Data acquisition

The methodology for pulse generation and data acquisition is similar to that described previously (Llano et al., 1988; Vandenberg and Bezanilla, 1991a). The patch clamp, either a Dagan 3900 Integrating Headstage (Dagan Corp., Minneapolis, MN) or a List EPC7 (Medical Systems Corp., Greenvale, NY), was connected through a data acquisition system similar to the one described by Stimers et al. (1987) to either an IBM AT-compatible or an IBM Model 80 computer, respectively. Currents were filtered at 5 or 8 kHz with an eight pole Bessel filter. Digital data was stored on magnetic media or optical disks and analyzed off-line.

Data analysis

The procedure for data analysis has been well described previously by Vandenberg and Bezanilla (1991b) and Correa et al. (1992). Records were idealized after subtraction of capacitive transients. The half amplitude cri-

terium was used to determine opening and closing transitions. Sometimes data was filtered further (3–4 kHz) to avoid contamination by spurious events. Dead-time correction was used in the single-channel analysis.

The idealized data was analyzed with maximum likelihood estimation of the rate constants by the methodology described in detail by Horn and Lange (1983), Horn and Vandenberg (1984), and Vandenberg and Bezanilla (1991b). One cyclic and five branched Markovian kinetic models were examined (Korn and Horn, 1988; McManus et al., 1988). The models tested had a maximum of six states, of which two were open, two or three were closed, and one or two were inactivated. Eight sets of data at six potentials (–40, +40, +60 (two sets), +80, +100 (two sets), and +110 mV) were evaluated. The computer program used in the analysis was kindly provided by Dr. Richard Horn (Thomas Jefferson University Medical College, Philadelphia, PA) and included dead-time correction following the method of Roux and Sauve (1985). The program was modified to run in an Intel 860 processor (Microway, Kingston, MA). The value referred to as the relative log(likelihood) was calculated by subtracting the maximum likelihood of an arbitrarily chosen model from the rest. The Akaike's asymptotic information criterion (AIC) was used to rank the models (Akaike, 1974). The AIC index was calculated as follows:

$$\text{AIC} = 2[(\text{number of free parameters in a model}) \\ \times (\text{number of data sets}) - \log(\text{maximum likelihood})]$$

The model with the lowest AIC is better.

RESULTS

Single-channel events and ensemble averages

Illustrated in Fig. 1 are traces showing single channel activity recorded at +60 mV and +110 mV for 18-ms test depolarizations. The recordings were made under conditions of inverse gradient with high internal sodium. The records shown come from a patch with only one channel. Immediately apparent is the high frequency of reopenings found at these positive potentials. Not obvious, however, is the shape of the macroscopic current reproduced from single-channel activity like the one shown. In Fig. 2 representative ensemble currents obtained at various pulse potentials are plotted as the probability of being open as a function of time during the pulse (*noisy traces*). Positive test potentials went from +40 to +110 mV. For comparison, the ensemble obtained in the same patch at –40 mV is illustrated in the last panel. For quantitative details please refer to the figure legend. Upon depolarization the probability of opening rises very rapidly giving a very sharp rising phase to the ensemble current. It peaks within the first ms or two (see figure legend) and then, as expected, decreases rapidly to a nonzero level, the mag-

TABLE 1 Recording solutions

	Na ⁺	Cs ⁺	Mg ²⁺	Ca ²⁺	Cl [–]	F [–]	Glutamate [–]	EGTA-Cs ⁺	HEPES-Na ⁺
Bath Solutions									
0 K ASW	455		50	10	570				10
540 Na	545				540				10
270 Na	275				270				10
Pipet Solution									
535 Na	535	5			10	20	500	1	10

Concentrations are in mM. The external solutions were pH 7.6, and internal solutions were pH 7.3.

* EGTA titrated with CsOH.

† HEPES titrated with NaOH.

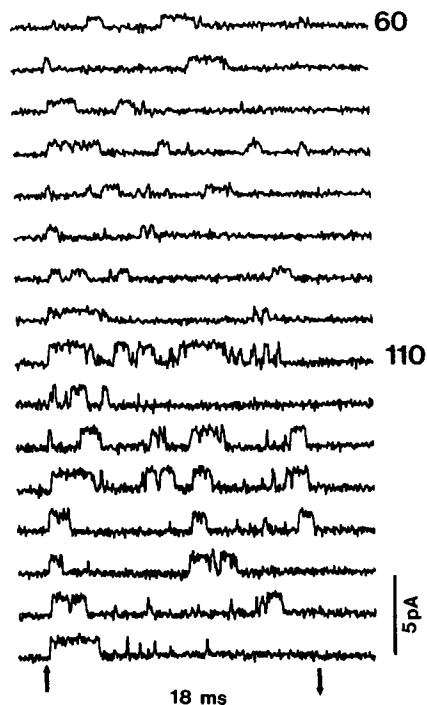


FIGURE 1 Examples of records showing single-channel activity at positive potentials, +60 and +110 mV. Onset and release of the 18-ms depolarization are indicated by the arrows at the bottom. Recordings were made at 5°C in 270 Na/535 Na. Data filtered at 4 kHz (+60 mV), and 5 kHz (+110 mV). Holding potential: -100 mV.

nitude of which increases with depolarization. The ratios of the current at the end of the pulse (I_{ss}) to that at the peak (I_{peak}) went from 0.14 at +40 mV to 0.3 at +110 mV. The I_{ss}/I_{peak} values were lower than those found in the dialyzed whole axons, which ranged from 0.2 at 0 mV to 0.5 at +100 mV. At +40 mV a hint of a rising phase is still present, but at +60 mV the current rises very fast. The ensemble at -40 mV shows the typical lag for sodium currents at negative potentials. The peak probability of opening reached the maximum of 0.70 at +80 mV. The time course of the onset of the current is further illustrated by the latencies to first opening. These are shown as the cumulative probability plots (*smoother curves*) superimposed on the $P(o)$ curves. At all the potentials, two components were found. At potentials more positive than +60 mV most of the openings occurred promptly after depolarization (about 90% within the first ms); longer first latencies become less frequent with increasing depolarization. Therefore the plateau phase of the current is mainly due to reopenings and not to late openings. At positive potentials, the average number of openings in traces with at least one opening was 10.44 ± 0.96 (mean \pm SE). At the two most extreme potentials, -40 and +110 mV, the averages were 2.2 and 12.7, respectively.

Open and closed times

The open and closed dwell times of the single-channel events for the experiment in Fig. 2 are shown in Fig. 3. Histograms

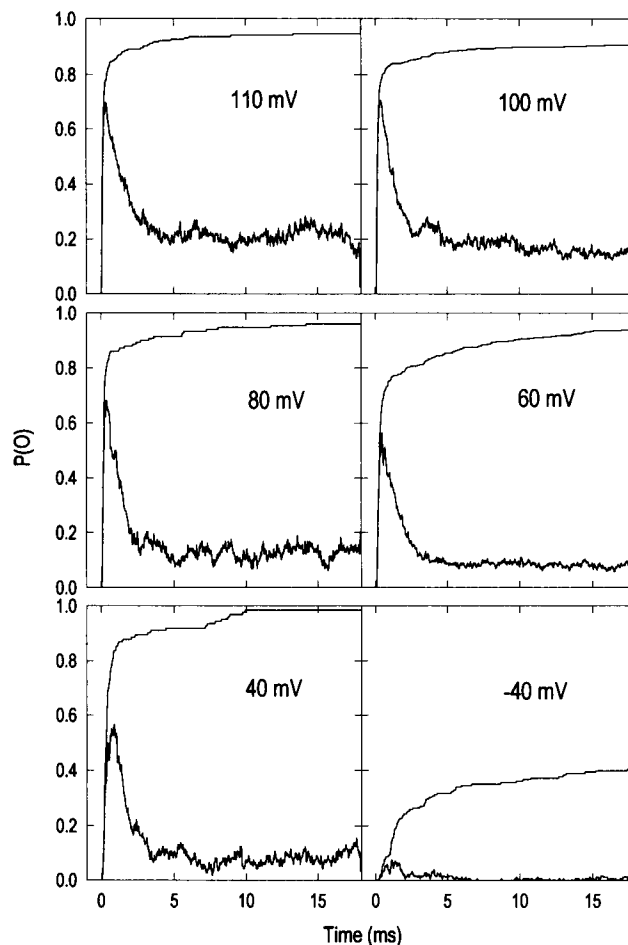


FIGURE 2 Probabilities of being open, $P(o)$, as a function of time during the pulse (*noisy traces*), and accumulated distributions of the latencies to first opening (*smoother traces*) from a patch pulsed to the following potentials: -40, +40, +60, +80, +100, and +110 mV. Following this same sequence of potentials, the number of records analyzed at each potential, and the corresponding average number of openings per trace with at least one opening (in parentheses), were as follows: 186 (2.2), 123 (6.9), 474 (7.1), 148 (10.7), 474 (10.9), and 201 (12). The peak probabilities of opening and times to peak were: 0.075 at 1.12 ms (-40 mV), 0.566 at 0.90 ms (+40 mV), 0.565 at 0.46 ms (+60 mV), 0.682 at 0.38 ms (+80 mV), 0.705 at 0.40 ms (+100 mV), and 0.697 at 0.36 ms (+110 mV). Approximate values for time constants of inactivation were obtained from the main component of a double exponential fit to the decay of $P(o)$ data at each potential. They were: 1.36 ms (-40 mV), 0.94 ms (+40 mV), 1.20 ms (+60 mV), 0.95 ms (+80 mV), 0.84 (+100 mV), and 1.19 ms (+110 mV). These values, and those of the times to peak $P(o)$ (see above) superimposed on data from dialyzed whole axons (not shown). Two additional sets of data from the same patch at +60, and +100 mV (not shown here), were used for maximum likelihood analysis; their number of records and average number of openings per trace (in parentheses) were: 150 (9.3), and 142 (11.1), respectively. Data was filtered at 3.5 kHz for data at -40 mV, 3 kHz at +40 mV, 4 kHz at +60 mV, and 5 kHz for all the rest. Recording solutions: 270 Na/535 Na. Temperature: 5°C. Patch: NBJN190C-J. Holding potential: -100 mV.

of open times are in the main panels; the corresponding shut time distributions are in the insets. These data were obtained from the analysis of a patch that during the recording time of approximately 1 h (33×10^3 transitions) did not show evidence of the presence of a second channel. The main fea-

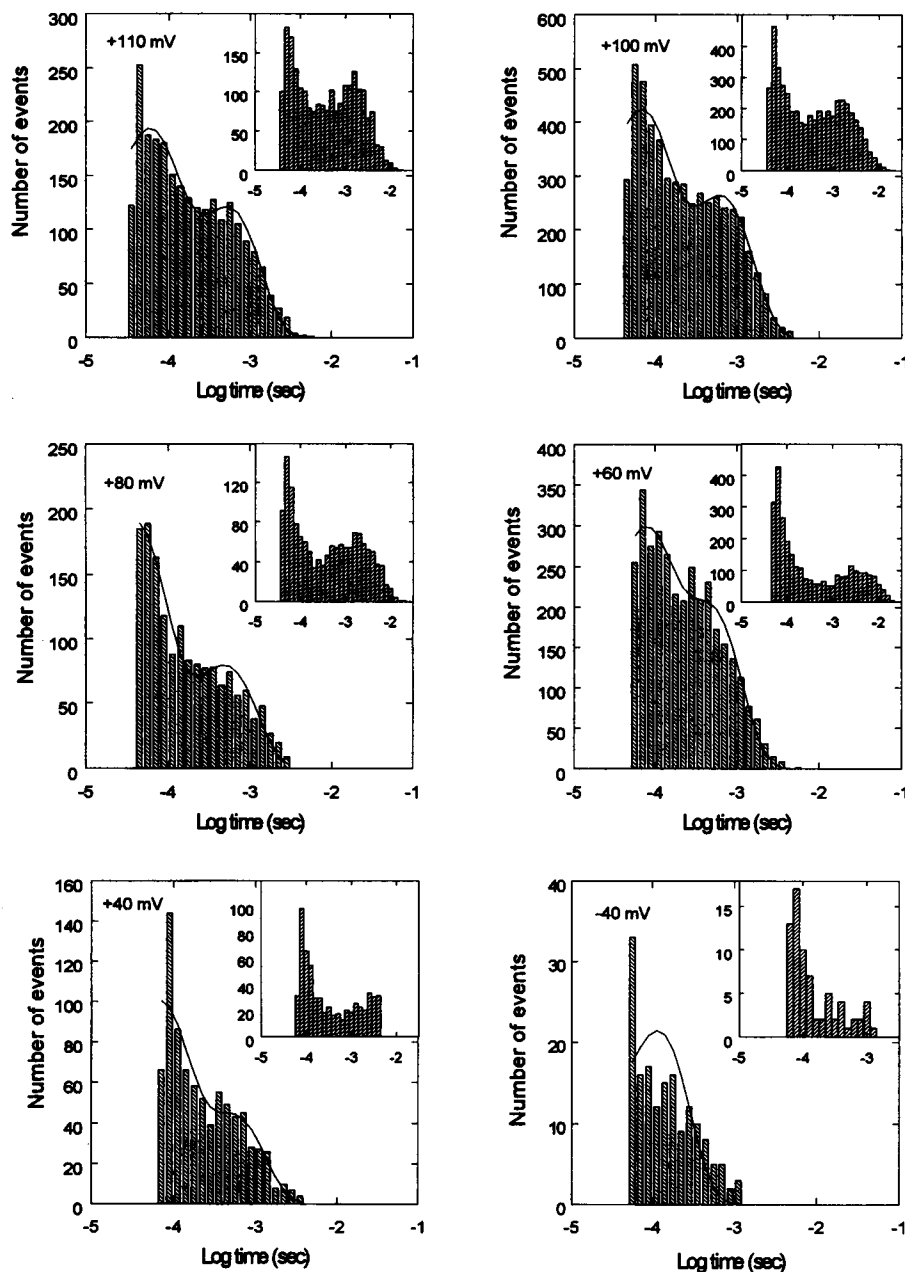


FIGURE 3 Open- and closed-time histograms. In each main panel are the distributions of open times classified in log bins of time (Sigworth, and Sine, 1987) for the same data as in Fig. 2. In each inset are the distributions of the corresponding closed times. The total number of transitions analyzed at each potential were as follow: 327 (-40 mV), 1650 ($+40$ mV), 6670 ($+60$ mV), 3156 ($+80$ mV), 10221 ($+100$ mV), and 4785 ($+110$ mV). The smooth curves are the fits of the open-time data to two exponentials. The fitted time constants (τ_1 and τ_2) and their corresponding weights (in parentheses) were the following: $\tau_1 = 408 \mu\text{s}$ (0.336) and $\tau_2 = 46.2 \mu\text{s}$ (0.664), at $+40$ mV; $\tau_1 = 354 \mu\text{s}$ (0.474) and $\tau_2 = 47.6 \mu\text{s}$ (0.526), at $+60$ mV; $\tau_1 = 381 \mu\text{s}$ (0.314) and $\tau_2 = 29.4 \mu\text{s}$ (0.686), at $+80$ mV; $\tau_1 = 495 \mu\text{s}$ (0.425) and $\tau_2 = 45.9 \mu\text{s}$ (0.576), at $+100$ mV; and $\tau_1 = 522 \mu\text{s}$ (0.427) and $\tau_2 = 50.6 \mu\text{s}$ (0.573), at $+110$ mV.

ture from Fig. 3 is the appearance with depolarization of a second component in the distribution of open times. The solid lines are the fits to two exponentials. The weights of the exponentials were comparable for all potentials (see figure legend), the fast component being on the average 1.6 times greater than the slow one. A small shift in weights from the fast to the slow component was seen as the potential was made more positive. The time constants also increased slightly with depolarization (see figure legend); this increase was more noticeable for the slower time constant. Overall, the main effect of depolarization was an increase in the number of events with slow open times. At least two components were always seen in the distribution of shut times (see insets).

Open times as a function of pulse length

We then proceeded to analyze the bursting activity to determine whether there was a different kinetic pattern evolving with time during the pulse. The rationale was that the burst durations and/or the open times could shorten after the first opening; this would give rise to a current that would inactivate more than what it would if the open times and/or burst durations remained the same throughout the depolarization. The analysis is illustrated here for $+60$ and $+100$ mV. First we looked at the open times of the channel as a function of time during the pulse. An arbitrary time, $T_{1/2}$, which refers to the average time during a pulse at which half

of the openings have taken place, was used to separate the data in two groups. The probability of a channel having a dwell time smaller than a given time is plotted as a function of time in Fig. 4. The solid lines represent data from the openings that occurred before $T_{1/2}$, and the dashed lines represent those occurring after $T_{1/2}$. At +100 mV the events tended to be longer and the curves shallower than at +60 mV. For both +60 mV and +100 mV, the open times after $T_{1/2}$ (4.6 and 5.8 ms, respectively) were shorter. The significance of the differences was verified applying the test for homogeneity of parallel samples (Rao, 1973, p. 399) to the density histograms. The differences were found to be significant at the 0.5% level for events lasting up to at least 2 ms. The χ^2 values (degrees of freedom) were 163.7 (92) at +60 mV and 241.9 (99) at +100 mV.

To see if there was a time dependence in the activity of the channel during the bursts, we calculated the probability of being open as a function of time within the burst, having that the channel opened at time zero, $M(t)$. To do this, bursts were aligned to set zero time at the time the channel first opened in the burst (Horn and Vandenberg, 1984). Bursts were defined as the period of activity starting with the first opening and ending with the last closing or the end of the pulse (whichever occurred first). The results are shown in Fig. 5

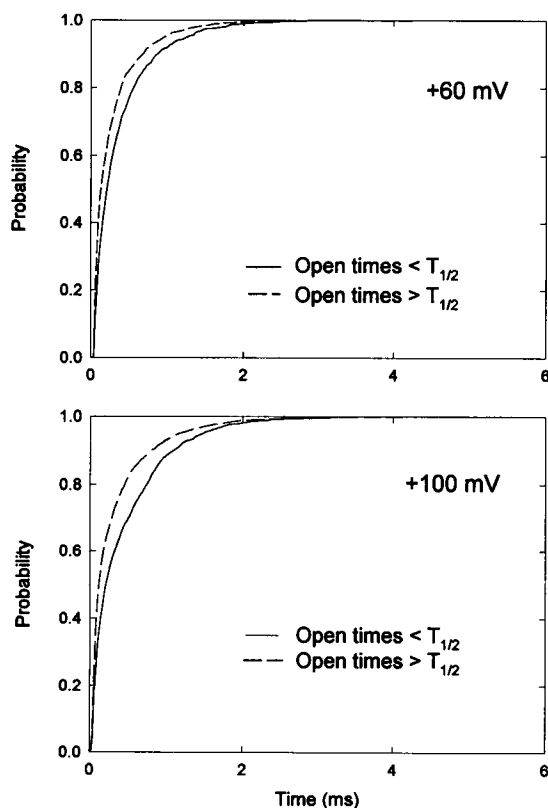


FIGURE 4 Accumulated probability of open times lasting less than the time in the abscissa, at +60 mV (top) and +100 mV (bottom). The events were separated into before and after an arbitrary time $T_{1/2}$, which is the time at which half the openings have occurred (Horn and Vandenberg, 1984). The $T_{1/2}$ values were 4.6 ms at +60 mV and 5.8 ms at +100 mV. Solid lines are the open times of events before $T_{1/2}$, and the dashed lines are those after.

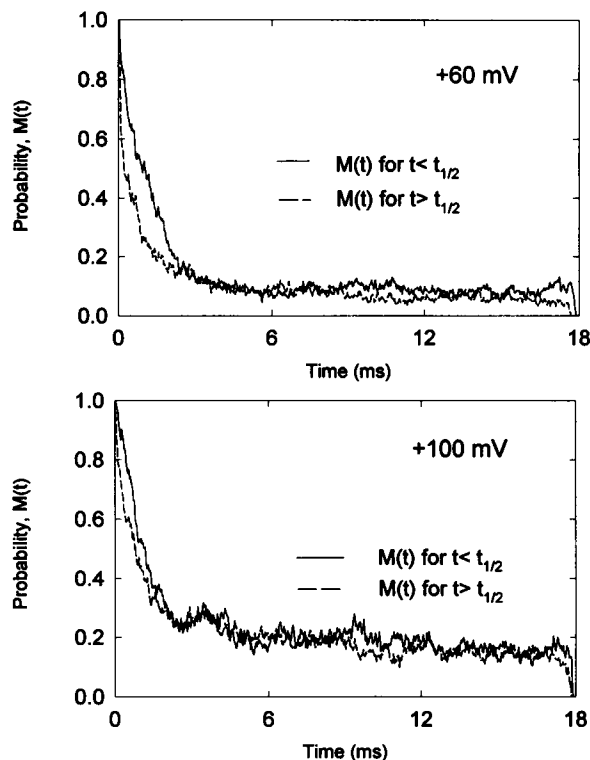


FIGURE 5 $M(t)$ distributions at +60 mV (top) and +100 mV (bottom). The probability of being open as a function of time was calculated after alignment of all the traces taking the time at which the channel opens for the first time as $t = 0$. An arbitrary time $t_{1/2}$, the average time at which half the first events opened, was used to separate the traces into two groups, before (solid lines) and after (dashed lines) $t_{1/2}$. The values of $t_{1/2}$ at +60 mV and +100 mV were 0.29 and 0.18 ms, respectively.

for +60 mV (top) and +100 mV (bottom). Again bursts were separated by their times of appearance; in this case, before and after the time half of the first openings had occurred ($t_{1/2}$). The respective values for $t_{1/2}$ at +60 and +100 mV were 0.29 and 0.18 ms. Except for the first 3 ms, there was no difference in the probabilities of being open between populations at both potentials. At +60 mV, after about 4–5 ms the probability attained a value close to 0.1 and stayed constant with time within the burst. The density histograms of $M(t)$ were tested for homogeneity giving χ^2 values (degrees of freedom) of 121 (99) up to 2 ms ($0.05 < p < 0.1$) and 41.24 (100) between 2 and 4 ms ($p > 0.995$). According to this, the two populations are different for the first 2 ms (at the 1% level), the difference being lost thereafter. At +100 mV the probabilities decayed faster than at +60 mV, to a higher level close to 0.2, and became constant only around 6 ms. For the first ms, the probability of being open seemed slightly higher for bursts initiating at $t < t_{1/2}$. The difference was not significant, however; the homogeneity test applied to the density histograms gave a χ^2 (d.f.) of 31 (100) for the first 2 ms ($p > 0.995$). These results taken along with the results from Fig. 4 indicate a tendency for the first event(s) in the bursts to be longer and to occur early in the pulse. Also, with increasing depolarization there is a tendency for bursts to last the length of the pulse (data not shown), thus the higher

probability steady level at +100 mV. Another approach to looking at the time dependence of the activity was to analyze the dwell times in closed and open states and their relationship with time of depolarization.

In Figs. 6 and 7 such an analysis is shown for data at +100 mV. At the other potentials the findings were the same. Quantitative details are in the figure legends. Except for the first openings, no correlation was found between the time of opening and the duration of the events. This was true for the data at real time (Fig. 6A), as well as, after alignment of the first opening events ($M(t)$ distribution, not shown). Also, at all potentials the events opening in the first 0.5 ms significantly outnumbered those opening during the rest of the pulse (Fig. 6B). There was, however, a small but consistent decline in the number of openings during the pulse. Clearly, the first event(s) behaved differently than the rest. There was an obvious and consistent correlation between the duration of the first event and the latency to the first opening (Fig. 7A). Openings were longer at the very beginning of the pulse and

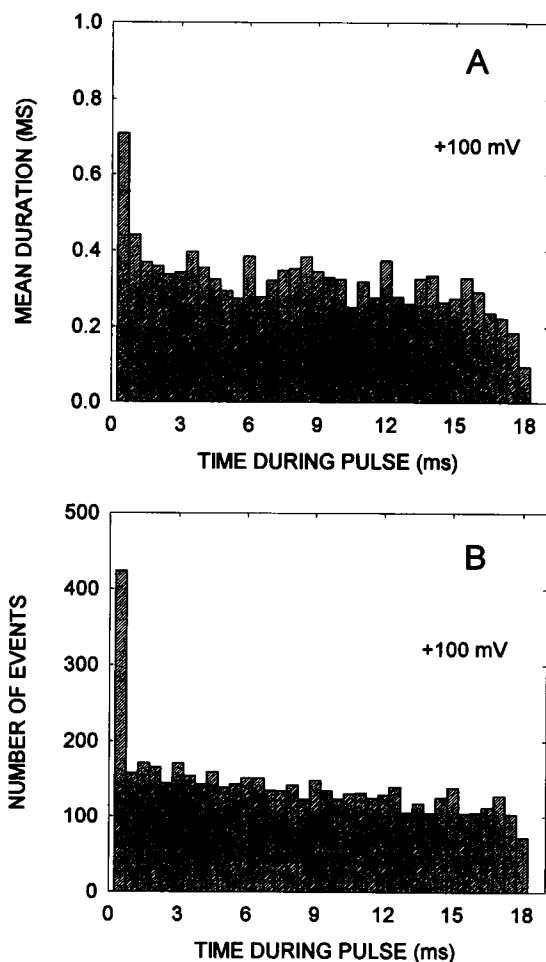


FIGURE 6 Analysis of average open times and opening frequency as a function of time during the pulse. The pulse potential was +100 mV. (A) The average values of open times of the events separated according to the time of opening in 500- μ s bins; (B) The number of openings along the pulse, grouped in bins of 500 μ s. The total number of openings was 5145. NBJN190H.

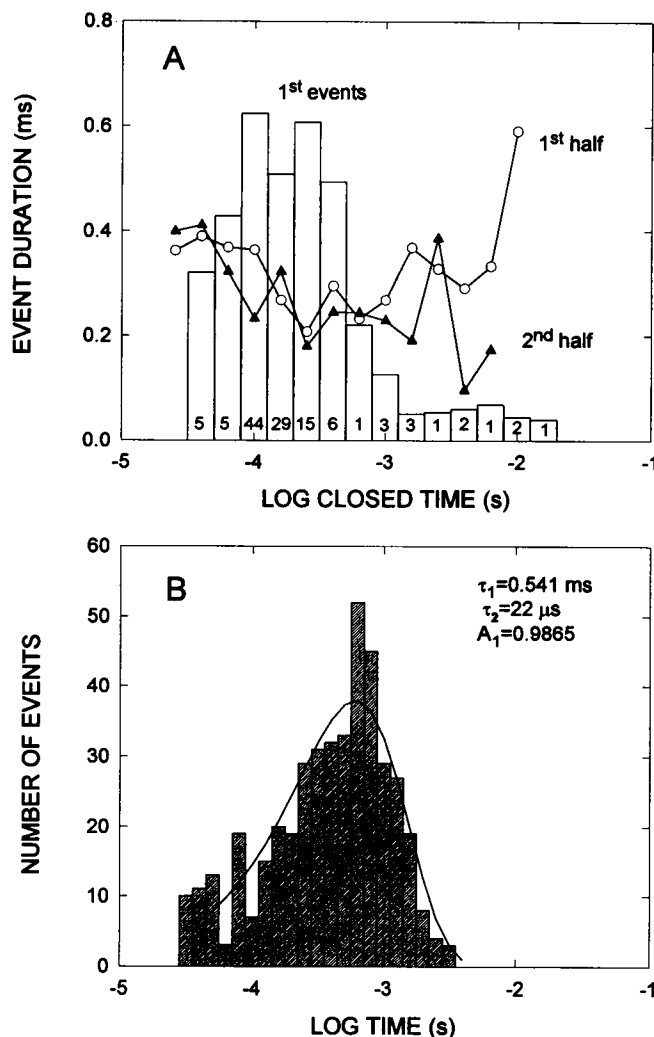


FIGURE 7 (A) Correlation between open and closed times. Plotted are the average open times classified in logarithmic bins of the closed time immediately preceding the opening event. In the bars are the average open times of the first events only; the corresponding closed times are the first latencies. The number at the bottom of the bars is the number of events per bin. In symbols are the average open times for the rest of the events separated in first (circles) and second (triangles) halves of the pulse, respectively. Total openings: 1581. NBJN190C; (B) The distribution of open times of first events only. The solid line is the fit to two exponentials. The time constants and weights of each component were: $\tau_1 = 541$ μ s (0.987) and $\tau_2 = 22$ μ s (0.014). Total openings: 5145. NBJN190H.

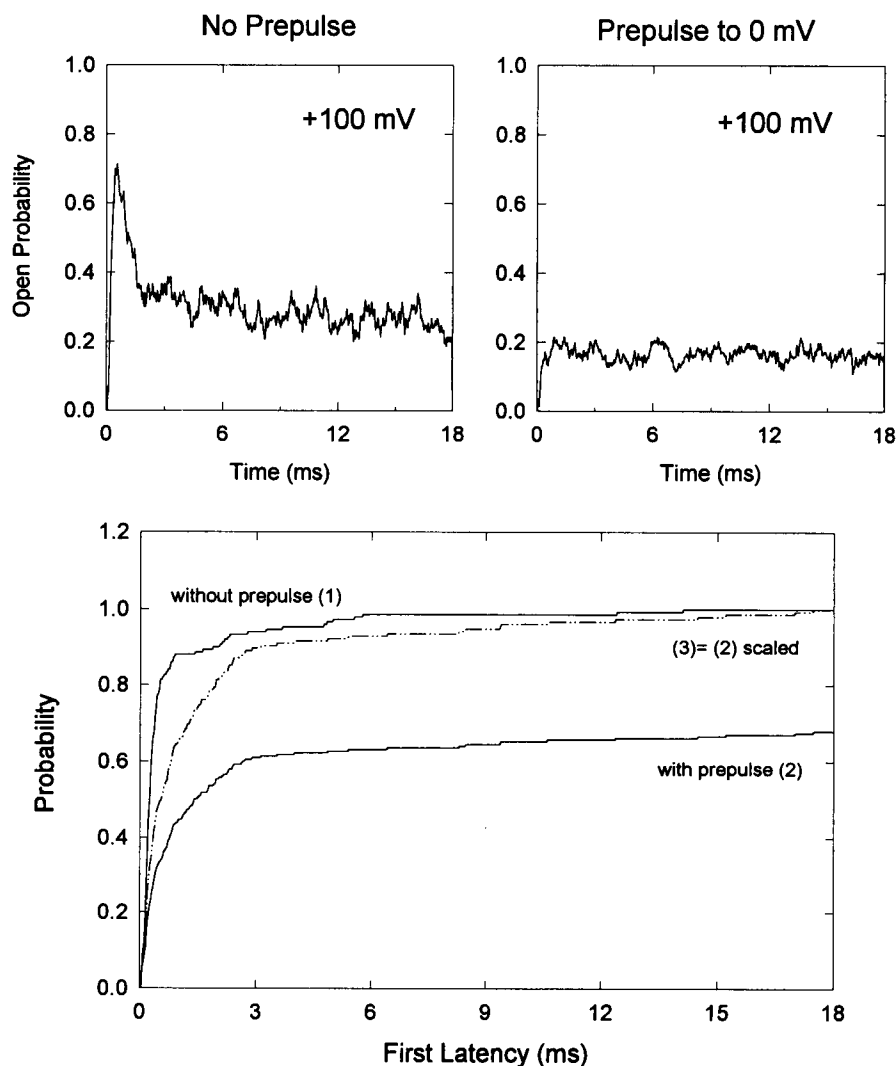
clearly shorter if the latency was long. First events were always short if opening late within the depolarization. This is illustrated in Fig. 7A where the average open times are correlated to the previous closed time classified in log bins. The bars are average open times of first events only, that is, the open times of the first events correlated to their first latencies. The symbols are data from all the other events separated in two: those occurring before (circles) and after (triangles) half the pulse length. For first openings only, few events were associated with long first latencies, and those were always very short. For events during the first half of the pulse there was a slight negative correlation with closed

times; however, the trend is lost for very long closures. Although the events clustered around short closed times, the average open time was fairly constant irrespective of the length of the previous closed period. At the other potentials we saw, however, there was a more consistent decay in the open times for longer closures. For the second half of the pulse there was more of a decline in the average open time with the length of the preceding closed times. The important issue is that the correlation is similar for first and second halves. Fig. 7 *B* shows a dwell time histogram of the open times of the first events only. As seen here for +100 mV, the distribution of the first event durations can be described by basically only one exponential. In the figure the solid line is a fit to two exponentials with τ_1 , τ_2 , and their weights as shown (also in figure legend). The slower component clearly dominates the distribution constituting 98.7% of the area. These results show that most of the time the channels open soon after depolarization via the same open state, its dwell time being slightly longer than for the rest of the events. We also consistently found that after a set of consecutive blanks single openings or re-initiation of activity were always with long latencies and short events (not shown).

Double-pulse experiments

In a typical Markovian process the dwell times in a particular state are determined by the transitions exiting that state. The closed times within the burst and between bursts should arise from transitions into any of the neighbor nonconducting states, be it closed, inactivated, or closed-inactivated. To explore further the relative positions of the suspected two open states, we investigated the effect of forcing the channel into the inactivated state. The single-channel activity at very positive potentials was recorded with double-pulse protocols in which the test pulse was preceded by a depolarizing prepulse. Figs. 8, 9, and 10 show the results. First, the probability of being open as a function of time during the pulse is shown in Fig. 8 for tests pulses to +100 mV with (*top right*) and without (*top left*) a depolarizing prepulse to 0 mV. As seen in the macroscopic currents with dialyzed axons (see Fig. 1, accompanying paper), the effect of the prepulse was to reduce or eliminate the fast inactivating component of the current here depicted as the initial transient increase in the opening probability. Also, with the prepulse, the steady-state probability was slightly reduced from about 0.3 to 0.2. An

FIGURE 8 Effect of a prepulse to 0 mV on the single-channel behavior at +100 mV. The top part of the figure shows the $P(o)$ at +100 mV with (*right panel*) and without (*left panel*) a 50-ms prepulse to 0 mV. Pulses were separated by a 1-ms repolarization period at the holding potential of -100 mV. The data without a prepulse is comprised of 3874 transitions from 150 records with an average of 13 openings/record (no blanks). With the prepulse to 0 mV, the average openings/record (with at least one opening) was 12.5. The number of transitions evaluated was 3827 and came from a set of 228 records, 73 of which were blanks. The bottom part of the figure shows the accumulated distribution of latencies to first opening. The smooth curves are the actual data without [*curve(1)*] and with [*curve(2)*] the prepulse. The dashed line, curve (3), corresponds to curve (2) scaled to match curve (1) at the maximum. Temperature: 4.2°C. NAJL251A.



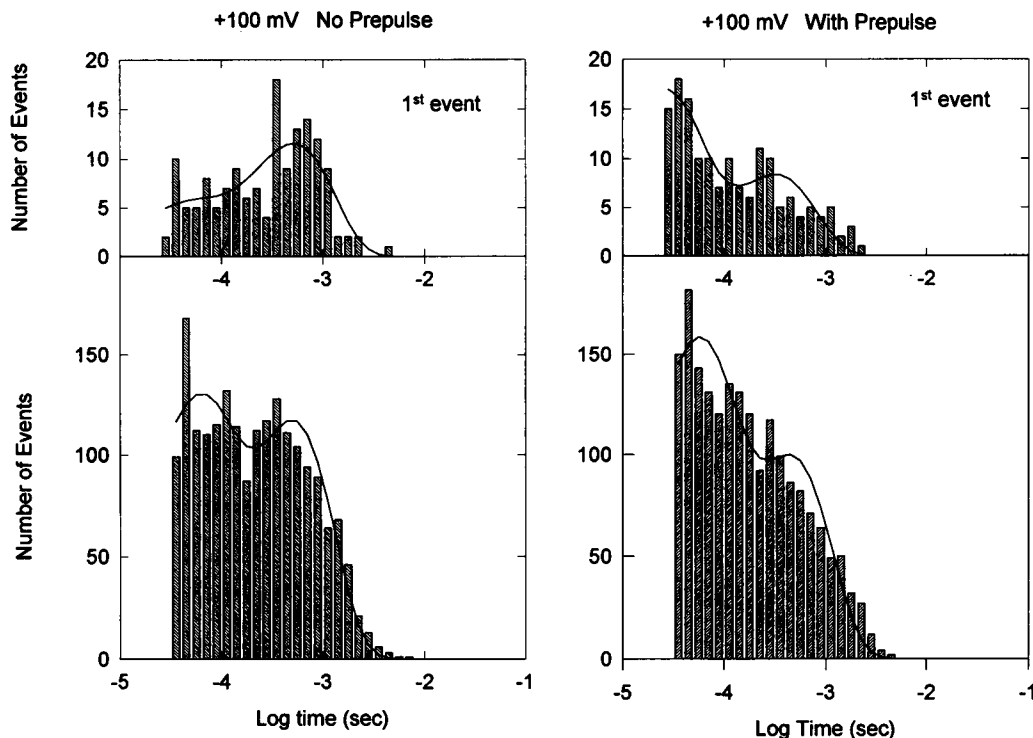


FIGURE 9 Open-time distributions with (*right panels*) and without (*left panels*) a prepulse. The data is from the same set as Fig. 8. The main panels at the bottom are the distributions of all the events classified in log bins of time. The top panels are the distributions for the first events only. The smooth lines are fits to two exponentials. The fitted time constants (mean \pm SE) and coefficients without a prepulse were: for all the events, $\tau_1 = 504 \pm 40 \mu\text{s}$ (0.542) and $\tau_2 = 48 \pm 6 \mu\text{s}$ (0.458); for the first events only, $\tau_1 = 521 \pm 73 \mu\text{s}$ (0.773) and $\tau_2 = 33 \pm 24 \mu\text{s}$ (0.227). The corresponding values for the data with a prepulse were: all the data, $\tau_1 = 449 \pm 45 \mu\text{s}$ (0.433) and $\tau_2 = 48 \pm 5 \mu\text{s}$ (0.567), and, for first events only, $\tau_1 = 318 \pm 47 \mu\text{s}$ (0.354) and $\tau_2 = 24 \pm 4 \mu\text{s}$ (0.646).

equivalent number of openings was used in the analysis (see fig. legend). For the data without a prepulse this was attained in a set of 150 records with no blanks. For the data with a prepulse, 228 records were used, of which 32% were blanks. This per se explains the lower level of steady-state open probability. The average number of openings/record with at least one opening were 12.5 and 13 with and without the prepulse, respectively. In the ensemble current obtained with the prepulse the steady-state level was achieved soon after the onset of the depolarization (within the first ms). The rising phase of the probability was faster in the absence of the prepulse, suggesting a slightly delayed first latency when subjected to previous depolarization. The latencies to first opening are illustrated at the bottom of the figure, as the accumulated probability of a channel opening before the time specified in the abscissa. Curves 1 and 2 represent the data without and with the prepulse, respectively. In the absence of a prepulse, the first latency has two obvious components: a very fast rise followed by a small, slow creep. Again, this essentially says that at +100 mV the majority of the channels open promptly after the depolarizing step. In addition there exists a population of channels that open late in the pulse, but they account for a small proportion of the total. The probability of a channel having opened at all was one. In contrast, with a depolarizing prepulse there was a slower rise in the probability, and the maximum level achieved in this patch

was close to 0.7, indicating a considerable number of traces (32%) without any openings. The differences in the time courses of activation are better resolved scaling curve 2 to curve 1. The first latencies at +100 mV after a depolarizing prepulse followed an almost monoexponential time course. The open state reached under these conditions takes longer to develop. This could be due to a delay produced by the movement among closed-inactivated states (see Scheme in the Discussion) populated during the 1-ms interpulse repolarization at -100 mV. The lag in the first latencies after a prepulse could also indicate a slow rate entering the second open state. So, if the inactivated state is forced onto the channel (with a prepulse), unless the rate of return from the inactivated state to the open state is considerable, a second open state can be reached from the inactivated state. This agrees well with the data from macroscopic ionic and gating currents in that inactivation follows a normal time course even though ionic current inactivation is incomplete (accompanying paper).

Shown in Fig. 9 are the open-time histograms obtained from the data in Fig. 8. Solid lines are the fits to two exponentials (the fitted values are in the figure legend). The effect of applying a depolarizing prepulse on the open time distributions at +100 mV was an apparent shift in the distribution of long open times toward shorter times (*bottom panels*). None of the two components disappeared com-

FIGURE 10 Probability, $M(t)$, of being open as a function of time after the first opening. Traces were aligned, taking time = 0 as the time the first opening occurs. The solid line is the data at +100 mV without the prepulse to 0 mV, and the dashed line is the data with the prepulse. It has the same data sets as in Figs. 8 and 9.

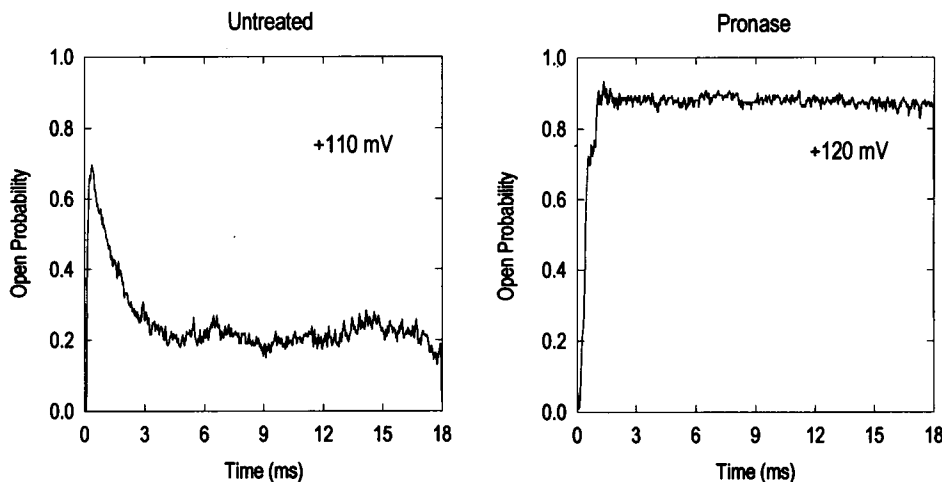
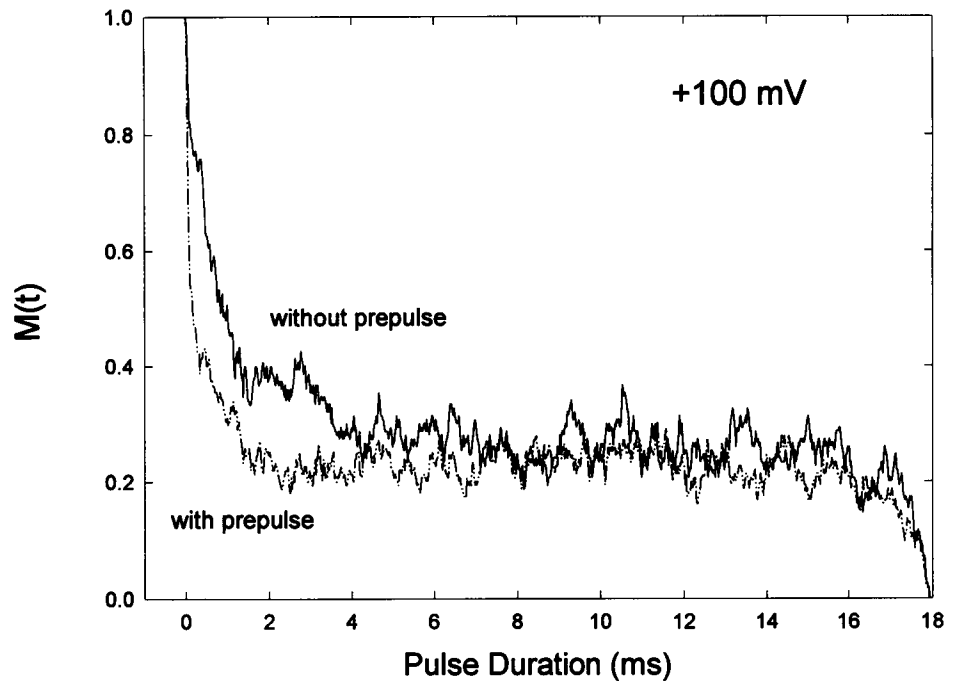


FIGURE 11 Effect of pronase treatment on $P(o)$. In the right panel is the $P(o)$ as a function of time during the pulse to +120 mV in a patch excised from an axon pretreated with pronase (2 mg/ml) for 30 s. The ensemble is from 131 records, with 1366 transitions. Temperature: 4°C. Holding potential: -100 mV. NAJL121E. For comparison, in the left panel is the $P(o)$ at +110 mV in a patch excised from an untreated axon.

pletely; instead, there was a switch in their weights with short events contributing more. The closed dwell time distributions were not significantly affected by the prepulse (not shown). Considering that with the interpulse repolarization of 1 ms to -100 mV some of the channels (about 20%) will have returned from inactivation, it is reasonable to find elements of both components. The Two-Tailed Test (Spiegel, 1961, p. 169) was used to evaluate the differences in the time constants between the data with and without a prepulse. τ_1 and τ_2 were not different at the level of significance (α) of 0.1 ($z = 0.922$ and 0.015 , respectively). The graphs at the top of Fig. 9 are the open-time distributions of the first events only (details in figure legend). Without a prepulse, the slow component of the distribution contributed more than 77% of the area. With the prepulse, the slow component became smaller (35%). The τ_1 and τ_2 of the distributions of first

events with and without a prepulse were not different at the 0.01 ($z = 2.331$) and 0.1 ($z = 0.362$) levels, respectively. When compared with the whole of the population, without a prepulse the time constants of the distributions of first events were not different at $\alpha = 0.1$ ($z = 0.195$ for τ_1 and $z = 0.617$ for τ_2); with a prepulse, τ_1 was not different at $\alpha = 0.01$ ($z = 2.019$) but the difference in τ_2 was significant even at $\alpha = 0.002$ ($z = 3.814$).

Burst analysis was also performed, and the results are shown in Fig. 10. Thin and thick lines are the $M(t)$ distributions of the data with and without the prepulse, respectively. When preceded by a depolarizing prepulse the steady level in the probability of being open is achieved earlier. The value of $M(t)$ at the steady level was the same for both sets of data, whereas the early components of $M(t)$ differ. The density distributions were found to differ for at least the first 0.5 ms

χ^2 (d.f.) of 35 (25) ($p < 0.1$). No difference was found thereof. Equal steady level probabilities are expected, because, for the $M(t)$ distribution, only traces with events are considered. The results confirm that the long-lived open state is populated only transiently and that with the depolarizing prepulse the corresponding events occur during the prepulse and do not appear again with the second pulse. These results resemble those shown in Fig. 5 of data separated in groups before and after $t_{1/2}$. It is as if with the prepulse we were looking at the population of events after $t_{1/2}$.

Effect of pronase

The results presented so far pointed toward two distinct open states that become obvious at very positive potentials with conditions of inverse gradient. At the potentials used in regular squid axon single-channel experimental protocols, i.e. more negative than +10 mV, the single-channel data can be accommodated by a kinetic scheme with only one open state. The appearance of a second open state at very positive potentials calls for further investigation of its location in a multiple-state kinetic scheme. We explored the relationship between the inactivated states and the open states by performing single-channel experiments in pronase-treated axons. Appropriate pronase treatments eliminate sodium channel inactivation without altering its activation (Stimers et al., 1985). Overtreatment with pronase slows activation, an effect that is due to the appearance of events with larger single-channel conductances and different kinetics (Levis, 1988). If the second open state were connected to the inactivated state, elimination of the latter with pronase should eliminate the former. Fig. 11 shows the probability of opening as a function of time during an 18-ms depolarization to +110 mV (untreated) and to +120 mV (pronase treated). The patch from an untreated axon displayed the previously observed kinetics of fast activation, prompt peak, and fast but incomplete inactivation mentioned above. The probability curve obtained in the patch from an axon treated with pronase showed rapid activation and no evidence of fast inactivation. Although the pulse potentials shown are not the same, they are both in the range of potentials where the probability of opening is expected to be reaching a maximum. If the second open state were to derive from the state reached via fast inactivation, then the open-time distribution would differ from the control in that only one open-time distribution should be found after elimination of the inactivation pathway with pronase, if there is no communication between the two open states. After pronase treatment the mean open time was dramatically increased (not shown). This indicates that at these very positive potentials the major exit way from the open states is *via* inactivation. The open times were lengthened to such extent that pulses normally ended before the channel closed. As events that ended with repolarization were not considered in the construction of the histograms, the limited amount of data left made it hard to evaluate the number of components in

both open- and shut-time histograms. Data from longer pulses is lacking.

DISCUSSION

The work described in this and the accompanying paper contributes important information with respect to the characteristics of the squid sodium channel in a range of potentials rarely explored, i.e., at very positive potentials. The features described are also present at potentials closer to zero but are less evident. From the data presented in the accompanying paper (Correa and Bezanilla, 1994) it is clear that the strategy used of imposing an inverse orientation to the ionic gradient to be able to better resolve the single-channel and macroscopic currents does not affect the results. Although we do not completely eliminate a role played by an interaction between sodium ions in the inside with the gating machinery of the channel, we feel confident that the conclusions do not depend on such an interaction. The main findings were: (1) the activity of only one type of sodium channel in the squid giant axon reproduces the findings at the macroscopic level that as depolarization is increased, inactivation is progressively less complete; (2) the sodium channel of the squid giant axon has two open states; and (3) although apparently incomplete inactivation does occur, charge immobilization does take place.

Chandler and Meves (1970a) in an attempt to extend to more positive voltages the range of potentials in the study of the sodium conductance of squid axons found that at positive potentials sodium currents did not inactivate completely. The biphasic behavior of inactivation led them to propose the following hypotheses. The most straight forward explanation was that at positive potentials a second, noninactivating sodium conductance appeared. The alternative hypothesis was that at positive potentials the gating characteristics of sodium channels were modified, and as a consequence fast, inactivation was incomplete. The data presented here rules out two different sodium conductances: one that inactivates and another that does not. The results from the macroscopic current experiments in dialyzed axons presented in the preceding paper (Correa and Bezanilla, 1994) indicate that the characteristics in study do not depend on the direction of the flow of current (see also, Shoukimas and French, 1980). In this paper we have concentrated on data obtained with an inverse gradient to reproduce the observations at the single-channel level under ionic conditions as close as possible to the macroscopic current experiments. This also increases the signal-to-noise ratio, which improves the resolution of single-channel currents. Ensemble averages of data from single channels collected over several hundred records reproduced the macroscopic ionic behavior. The activity of a single channel could mimic the incomplete inactivation found in whole axons looking at about 10^9 channels at a time.

Biphasic inactivation in other preparations has been correlated with fast and slow gating modes (Patlak and Ortiz, 1986; Moorman et al., 1990; Zhou et al., 1991). In those

cases, the channel exhibits a behavioral pattern very different than the one observed in the squid. Fast and slow gating modes appear as short and long bursting behavior, sometimes involving changes in the dwell times, with the channel switching from one to the other gating mode, and may be subject to modulation (Zhou et al., 1991; Isom et al., 1992). In squid, the bursts are mostly long, and ensemble averages of these reproduce the macroscopic pattern. Runs analysis using the sign test around the median of the P_o (Bendat and Piersol, 1971, p. 122) was performed to evaluate the randomness of the probability of opening. For all the samples tested at different potentials and from at least two patches, the tests indicated no trends with time in the probability of opening ($\alpha = 0.05$). As was mentioned above (Results), a trend was observed when long stretches of successive blanks were found in between stretches of activity. In those cases, the run test confirmed nonrandomness, providing an internal control.

Analysis of the single-channel data put in evidence features not obvious in the previous work on the same channel by Vandenberg and Bezanilla (1991a, b); those experiments were done with the regular sodium gradient and in the range between resting potential and -20 mV. In the first place, we found a second component to the distribution of open times. This second component was not seen or at least not justifiable at negative potentials. As the results are obtained in patches with only one channel, on the basis of a Markovian interpretation of channel kinetics, this can only occur if the channel develops a second open state. A second open state (or conductance) has been previously suggested for the squid sodium channel (Chandler and Meves, 1970c; Bezanilla and Armstrong, 1977; Keynes, 1992) to explain certain features of its gating and conductance, but the evidence had not been conclusive. More than one open state has also been proposed based on single-channel recordings for sodium channels from N1E115 mouse neuroblastoma cells (Nagy et al., 1983; Nagy, 1987). The neuroblastoma channel differs from the squid channel in several aspects. The second open state of the neuroblastoma sodium channels was manifest at potentials between resting and -20 mV; two distributions were found in the amplitude histograms; and, the relative probability of finding events with shorter open times was higher early in the pulse (Nagy et al., 1983; Nagy, 1987). A similar pattern of longer openings late in the test pulse led Sigworth (1981) to propose the existence of a second open state in channels from the Node of Ranvier. In other preparations of unmodified sodium channels, however, only one open state has been found (cf. Quandt and Narahashi, 1982; Horn and Vandenberg, 1984; Scanley et al., 1990). On the other hand, closed times showed at least two components also expected from a multistep gating process. Secondly, it became clear that the channel reopens many times during a voltage step and that the reopenings, on the average, were more at positive than at negative potentials. Because most of the features modeled for the squid sodium channel at negative potentials (Vandenberg and Bezanilla, 1991b) are still present at positive potentials, our hypothesis is that the second

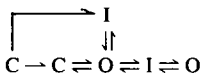
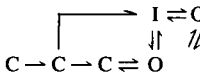
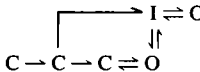
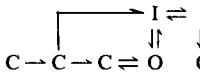
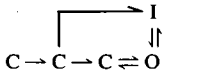
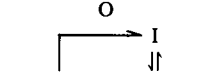
open state of the channel is only significantly populated at positive potentials.

Kinetic modeling

The rest of this discussion will concentrate on possible kinetic schemes that can account for the data at positive potentials. In Tables 2 and 3 we have listed a series of possible arrangements introducing a second open state in the basic model found by Vandenberg and Bezanilla (1991b) to best fit the data for the squid single sodium channel data. We will not enter into detailed analysis of the model other than for the inclusion of the second open state. For the other features refer to Vandenberg and Bezanilla (1991b).

There is no question that a series of closed states are required before going into an open state (i.e., Hodgkin and Huxley, 1952; Vandenberg and Bezanilla, 1991b). Several pieces of evidence, of which data from gating current experiments are probably the most conclusive, warrant the existence of many closed states (Armstrong and Bezanilla, 1977). When the membrane is held at a hyperpolarized potential, say -100 mV, most of the channels are expected to be populating closed states far away from the open conducting state. With depolarization the equilibrium is shifted toward a conducting configuration, and the first open state is populated. With a slight delay, fast inactivation takes place, and the channels become non-conducting again. Some channels, however, do not follow this pathway and access the inactivated state directly from one of the closed states. This route is of relevance at potentials close to the resting potential and also when exposed to a pre-depolarization, but with

TABLE 2 Ranking of kinetic models according to the AIC index

Model	Relative log(likelihood)	AIC	Convergence* (8 potentials)
S6 	339	1	-
S5C 	104	2	-
S5 	0	3	+
S1 	-117	4	-
S9 	-3275	5	-
S8 	-3701	6	+

* Only those models that converged for the full set have the + sign.

TABLE 3 Ranking of models that converged at all four data sets at -40 , $+60$, $+80$, and $+100$ mV

	Model	Log(lik)	AIC	Convergence (4 potentials)
S5	$\begin{array}{c} \text{I} \rightleftharpoons \text{O} \\ \updownarrow \\ \text{C} \rightarrow \text{C} \rightarrow \text{C} \rightleftharpoons \text{O} \end{array}$	0	1	+
S8	$\begin{array}{c} \text{I} \rightleftharpoons \text{O} \\ \updownarrow \\ \text{C} \rightarrow \text{C} \rightarrow \text{C} \rightleftharpoons \text{O} \rightleftharpoons \text{O} \end{array}$	-47	2	+
S6	$\begin{array}{c} \text{I} \\ \updownarrow \\ \text{C} \rightarrow \text{C} \rightleftharpoons \text{O} \rightleftharpoons \text{I} \rightleftharpoons \text{O} \end{array}$	-1805	3	+

stronger depolarizations the main route is via the open state (Vandenberg and Bezanilla, 1991b). During inactivation, the so-called "inactivating particle" interacts with the gating machinery, causing charge immobilization (Armstrong and Bezanilla, 1977). Upon repolarization the charge returns to its initial condition in a biphasic way. First, some charge, about $\frac{1}{3}$ of the total, returns with very fast kinetics, and then, as the inactivating particle leaves its docking or immobilizing site, the rest of the charge returns but with slower kinetics, the rate depending on the rate-limiting step (unbinding of the particle). The speed of recovery of the charge is very dependent on the potential for repolarization. When the membrane is taken to very positive potentials, not all the conductance is shut down during depolarization. What we have seen is that this steady level of current is mainly due to re-openings of the channels. One possibility is that there could be a significant return from inactivation; flickering would arise from successive transitions from the open state to the inactivating and the closed state. More than one open-time distribution would not support this conclusion, however. Another possibility is that after inactivation is established, the channel is capable of accessing a second open state from which it would reenter the inactivated state. This interpretation is consistent with data from single channels and from macroscopic ionic and gating currents. Our data from the dialyzed squid axons indicate that the second open state is probably accessed from the inactivated state, inasmuch as fast inactivation was found to proceed normally and charge immobilization was not affected at positive potentials. A second open state emerging from the inactivated state would be analogous to the proposal, in terms of conductances, made by Chandler and Meves (1970c) and by Bezanilla and Armstrong (1977) for the squid axon. The arrangement proposed by Sigworth (1981) for the Node of Ranvier and that by Nagy (1987) for N1E115 cells differs in that the first and second open states stem in parallel from resting states. More than one open state had been previously proposed for the batrachotoxin (BTX)-treated squid sodium channel (Correa et al., 1992). In that case, the distributions of open times showed at least three components. Interestingly, Tanguy and Yeh (1988) have reported that in the squid axon, although BTX eliminates fast inactivation, charge immobilization still pro-

ceeds, suggesting that BTX may modify the inactivated state making it conducting.

Keynes et al. (1992a) have found in the dialyzed squid giant axon differences in the Q_{10} for sodium permeability at the peak and at steady level. Assuming no kinetic complications in the determination of the permeability at the peak, two different pathways in the conduction process, each with different temperature dependencies (energy of activation), could be proposed. If we assume that the channel actually goes first to an open state, as our data suggests, then inactivates and only then populates the second open state, there are pathways in such a scheme that would not be shared; hence, it is not difficult to imagine differences in the Q_{10} s. We have not seen a difference in single-channel conductance between events occurring at different times during the pulse. In other cell types (see for example Nagy et al., 1983) this has been an argument in favor of a second open state. In our experiments, the sizes of the events were the same at the beginning and end of the pulse within the resolution of the system. It is important to point out the fact that our single-channel experiments were performed in the absence of external Ca^{2+} . As external divalents block the single-channel conductance with no effect on gating other than a surface charge-related shift in the voltage-dependent parameters (Vandenberg and Bezanilla, 1991a), it makes the conductance data from singles and from dialyzed axons not totally comparable. More studies on the conductance properties of the second open state along with the effect of internal ions are needed.

Maximum likelihood analysis

To decide on a more quantitative base among several possibilities of connection between first open, inactivated, and second open states, we used the maximum likelihood analysis of Horn and Lange (1983). The models shown in Table 2 all have at least two closed states before an open state. Single-channel data are not sensitive to events occurring far away from the open states, thus the reduced number of closed states in the models presented, which were tested with single-channel data only. Also, although the data suggest that the access to the second open state happens after transit through the first open state, model S9 (Table 2), where the two open states evolve from the last closed state, was also tested. In Table 2 six models are compared. They have been ordered according to the AIC index (see Materials and Methods), which takes into account the log(likelihood), the number of free parameters and the number of data sets. In this classification no demand was made on convergence at all potentials and data sets (convergence was assessed when it was possible to compute the covariance matrix). In column 4, the signs indicate those that converged for all the data sets (+ signs) and those that did not converge for at least one data set (− signs). The most favored scheme (model S6) was that with the highest relative log(likelihood) (column 2). However, the rate constants predicted by this model did not show consistency, in that there was no clear trend in their voltage dependencies or in their magnitudes. Between two consecu-

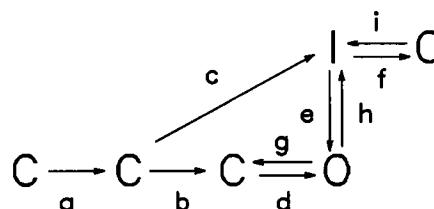
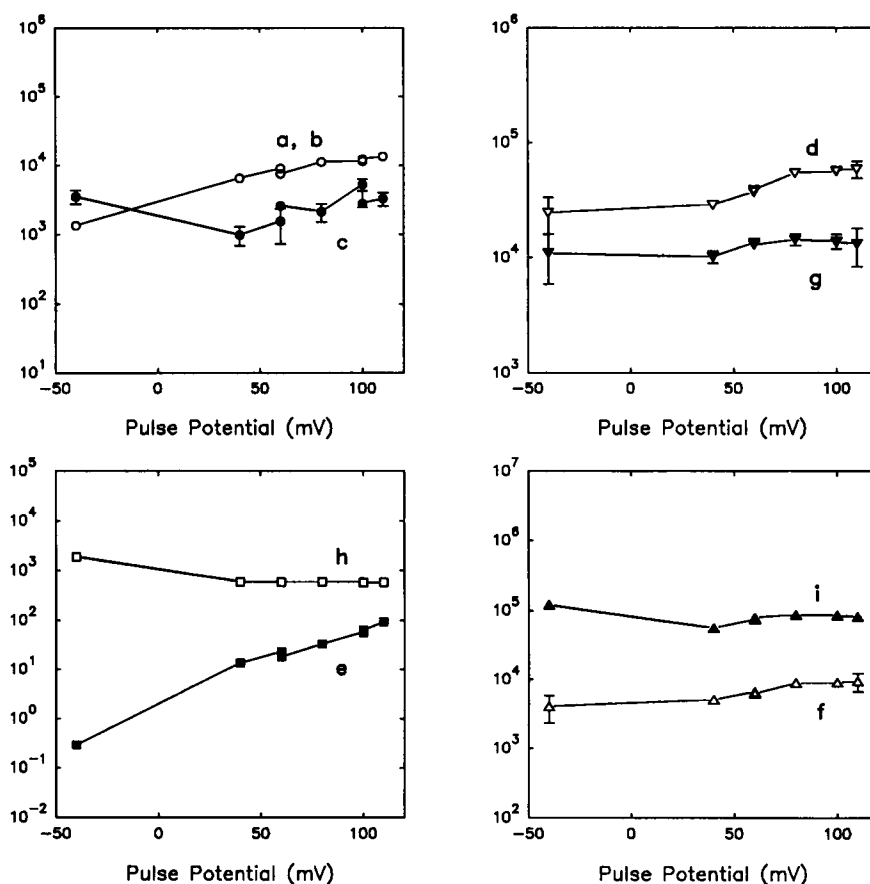


FIGURE 12 Model S5 and fitted rate constants. The top part of the figure shows Model S5 with the rate constants for the individual transitions between states in small letters, *a* through *i*. The plots at the bottom represent the voltage dependencies of the rate constants as fitted by the maximum likelihood analysis. Note that the ordinates are s^{-1} plotted in log scale.



tive voltages the model sometimes produced changes that differed in orders of magnitude in their rate constants. Another example of lack of consistency was that for two sets of data at +60 mV, Model S6 made the activation pathway go uniquely through the inactivated state for one set and only through the regular route for the other. The second best model: S5C, is an extension of model S5 (third in preference) in which the two open states are connected. This model had two more parameters to fit and did not reach convergence at any potential. It is hard to evaluate the model on this basis, although it seems very plausible. Models S1, S9, and S8 had far less likelihood. S1 differs from S6 in that the second inactivated and second open states are now evolving from the inactivated state and not from the first open state. S9, as stated before, allows the two open states to be accessed from the last closed state. This, as expected, had a very poor likelihood. The single-channel data clearly showed that upon depolarization the first opening shows only one dwell-time

distribution, indicating that the first time the channels open they do it through only one open state. The second open state had to follow. Finally, S8 where the second open state directly follows the first, had the worst ranking. The gating current experiments had suggested that the second open state would be accessed after the development of fast inactivation. It was, therefore, not surprising to find a poor likelihood for this model.

In Table 3, three of the models are compared, but this time the requirement of convergence at the same potentials is applied. All three models showed convergence in four data sets (-40, +60, +80, and +100 mV). Model S6, which previously had the highest ranking, was the worst. This model had shown no consistency in the predicted magnitude and voltage dependence of the rate constants taking all the data into account. Model S8, which ranked worst before, is now comparable to S5. Interestingly, a combination of the two models (S5 and S8) would give rise to the cyclic model S5C in

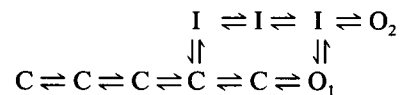
Table 2. Model S5 had the highest ranking. Actually, for all the comparisons where convergence was a requirement, irrespective of the number of data sets involved, S5 always ranked highest in log(likelihood), according to the AIC index. Although the model is oversimplified, the main features agree with the experimental data.

In Fig. 12 we have plotted the predicted values for the rate constants in model S5 according to the maximum likelihood analysis. The magnitudes of the rate constants are not to be taken at face value, because the model is undoubtedly an oversimplification. The value of the analysis is in its highlighting the trend and consistent behavior of the rate constants. Rates *a* and *b*, for simplicity, were set to be equal. No return was allowed between closed states or between the second closed and the inactivated state. As expected, rates *a*, *b*, and *c*, increase monotonically with depolarization at positive potentials. Rate *c* at -40 mV shows the tendency already mentioned above and in Vandenberg and Bezanilla (1991b) of populating the inactivated state directly from a closed state. The nonmonotonic behavior of *c* can arise from the lack of return among closed states. The transition from the last closed to the first open state described by rates *d* and *g*, in the forward and backward directions respectively, is also favored by depolarization at all potentials, with *d* showing slightly more voltage dependence than *g*. The next transition, between the first open and the inactivated states showed interesting features. As expected, rate *h* showed little or no voltage dependence, however, rate *e*, contrary to expectations, had an inverse dependence on voltage, increasing steeply with depolarization. In the extended model proposed by Vandenberg and Bezanilla (V-B model, 1991b), rate *e* decreased with depolarization, making the return from inactivation through the transition I-O1 less likely. The significant magnitude and voltage dependence of *e* could arise simply from the lack of an exit from the inactivated state toward the closed states, because there is no return from I to C. The V-B model accommodates several inactivated states running in parallel to the closed states closest to the open state. This parallel route is needed to account for the charge immobilization seen in gating current experiments. Lacking this, *e* has been given a more relevant role than expected. This, however, does not rule out some flicker occurring between first open and inactivated state. Finally, the rates of the transition between the inactivated state and the second open state, *f* and *i*, predicted very short open dwell times as was found experimentally. The backward rate was favored at all potentials but more so at -40 mV; the forward rate tended to increase with depolarization. An important consequence of having short open dwell times in the second open state is the influence of the filtering bandwidth during acquisition on the $P(o)$ at positive potentials. If, as predicted by the model, the open times of this open state are very short, a natural consequence of limited bandwidth is missed events. The ensemble probabilities would then be affected, showing a lower than expected level during the plateau. The ratios I_{ss}/I_{peak} from patch recordings were lower than those obtained in the dialyzed axons (accompanying paper; also, legend of Fig. 2),

where the recordings, made at 20–50 kHz bandwidth, would show a better estimation of the plateau current. One more aspect not to be overlooked, however, is the influence that the internal TEA, present in the dialyzed axon experiments, might have had on macroscopic inactivation.

A kinetic model for the squid axon Na⁺ channel

The analysis of the models discussed above gave a more quantitative basis to locate the relative position of the second open state. The models evaluated are, however, oversimplifications to facilitate the calculations by reduction of the number of parameters to fit. They were also designed to emphasize the contribution of the single-channel data, which refer to transitions near the open state. To account for the data provided by other experimental approaches, in particular, that from gating currents, the model needs obvious extension. Integrating our findings to what has been already proposed for the squid sodium channel, which was based mainly on data in the negative range of potentials, the following scheme emerges:



The sequence is essentially that of Vandenberg and Bezanilla (1991b) but with the addition of the second open state originating from an inactivated state. Our results also have contributed additional information that originated from the prepulse experiments in whole dialyzed axons. The gating current experiments with prepulses suggest that a substantial amount of charge is moved among the last closed states near the first open state and that it very likely corresponds to the slow component of the “on” gating current (see Correa and Bezanilla, accompanying paper). In addition, the kinetics of the charge movement among the final closed states was not equal to that moved in the route in parallel among the inactivated states. These results indicate that the rate constants between the I states are probably different than the rate constants between the last two closed and the first open states. In the model of V-B, they were assumed to be equal.

The studies by Keynes and collaborators, as mentioned above, suggest that the conduction properties of the channel in the second open state could differ from those of the first open state (Keynes et al., 1992a, b; Keynes and Meves, 1993). This might turn out to be very important at the molecular level, because the data reported in this paper suggest that the second open state, a conducting state, develops while the inactivating particle is interacting with its docking site. The strains on possible conformations that the protein may acquire under these conditions might, in fact, alter conduction properties. This contention is interesting enough to warrant further exploration. If any of the cloned sodium channels show a second open state under similar experimental conditions, the study of its properties can be pursued with and without inactivation, and site-directed mutagenesis may

help in locating groups involved in the establishment of this second open state.

This work was supported by USPHS grant GM30376.

REFERENCES

- Adelman, W. J., and J. P. Senft. 1966. Effects of internal sodium ions on ionic conductance of internally perfused axons. *Nature*. 212: 614–616.
- Akaike, H. 1974. A new look at the statistical model identification. *IEEE Trans. Automatic Control*. AC-19:716–723.
- Armstrong, C. M., and F. Bezanilla. 1977. Inactivation of the sodium channel. II. Gating current experiments. *J. Gen. Physiol.* 70:567–590.
- Bendat, J. S., and A. G. Piersol. 1971. Random Data: Analysis and Measurement Procedures. John Wiley & Sons, Inc., New York. 407 pp.
- Bezanilla, F., and C. M. Armstrong. 1977. Inactivation of the sodium channel. I. Sodium current experiments. *J. Gen. Physiol.* 70:549–566.
- Bezanilla, F., and A. M. Correa. 1991. Single sodium channels in high internal sodium in the squid giant axon. *Biophys. J.* 59:12a.
- Bezanilla, F., and A. M. Correa. 1992. Kinetics of Na⁺ channels at positive potentials. *Biophys. J.* 61:A270.
- Bezanilla, F., and C. Vandenberg. 1990. The cut-open axon technique. In *Squid as Experimental Animals*. D. L. Gilbert, W. J. Adelman, Jr., and J. M. Arnold, editors. Plenum Press, New York. 153:159.
- Chandler, W. K., and H. Meves. 1970a. Sodium and potassium currents in squid axons perfused with fluoride solutions. *J. Physiol.* 211: 623–652.
- Chandler, W. K., and H. Meves. 1970b. Evidence for two types of sodium conductance in axons perfused with sodium fluoride solution. *J. Physiol.* 211:653–678.
- Chandler, W. K., and H. Meves. 1970c. Rate constants associated with changes in sodium conductance in axons perfused with sodium fluoride. *J. Physiol.* 211:679–705.
- Correa, A. M., and F. Bezanilla. 1994. Gating of the squid sodium channel at positive potentials. I. Macroscopic ionic and gating currents. *Biophys. J.* 66:1853–1863.
- Correa, A. M., F. Bezanilla, and R. Latorre. 1992. Gating kinetics of Batrachotoxin-modified Na⁺ channels in the squid giant axon. Voltage and temperature effects. *Biophys. J.* 61:1332–1352.
- Goldman, L. 1988. Internal cations, membrane current, and sodium inactivation gate closure in *Myxicola giant axons*. *Biophys. J.* 54:1027–1038.
- Hamill, O. P., A. Marty, E. Neher, B. Sackmann, and F. Sigworth. 1981. Improved patch clamp techniques for high resolution current recording from cells and from cell-free membrane patches. *Pflugers Arch. Eur. J. Physiol.* 381:85–100.
- Hodgkin, A. L., and A. F. Huxley. 1952. A quantitative description of membrane current and its application to conduction and excitation in nerve. *J. Physiol.* 117:500–544.
- Horn, R., and K. Lange. 1983. Estimating kinetic constants from single channel data. *Biophys. J.* 43:207–223.
- Horn, R., and C. A. Vandenberg. 1984. Statistical properties of single sodium channels. *J. Gen. Physiol.* 84:505–534.
- Isom, L. L., K. S. De Jongh, D. E. Patton, B. F. X. Reber, J. Offord, H. Charbonneau, K. Walsh, A. L. Goldin, and W. A. Catterall. 1992. Primary structure and functional expression of the α subunit of the rat brain sodium channel. *Science*. 256:839–842.
- Keynes, R. D. 1992. A new look at the mechanism of activation and inactivation of voltage-gated ion channels. *Proc. R. Soc. Lond. B. Biol. Sci.* 249:107–112.
- Keynes, R. D., N. G. Greeff, and I. C. Forster. 1992b. Activation, inactivation and recovery in the sodium channels of the squid giant axon dialysed with different solutions. *Philos. Trans. R. Soc. Lond. Biol.* 337: 471–484.
- Keynes, R. D., and H. Meves. 1993. Properties of the voltage sensor for the opening and closing of the sodium channels in the squid giant axon. *Proc. R. Soc. Lond. B. Biol. Sci.* 253:61–68.
- Keynes, R. D., H. Meves, and D. Hof. 1992a. The dual effect of internal tetramethylammonium ions on the open states of the sodium channel in the squid giant axon. *Proc. R. Soc. Lond. B. Biol. Sci.* 249:101–106.
- Korn, S. J., and R. Horn. 1988. Statistical discrimination of fractal and Markov models of single channel gating. *Biophys. J.* 54:871–877.
- Levis, R. A. 1988. Single Na channel currents from squid giant axon following removal of fast inactivation by pronase. *Biophys. J.* 53:226a.
- LLano, I., C. K. Webb, and F. Bezanilla. 1988. Potassium conductance of the squid giant axon. Single channel studies. *J. Gen. Physiol.* 92:179–196.
- McManus, O. B., D. S. Weiss, C. E. Spivak, A. L. Blatz, and K. L. Magleby. 1988. Fractal models are inadequate for the kinetics of four different ion channels. *Biophys. J.* 54:859–870.
- Moorman, J. R., G. E. Kirsch, A. M. J. VanDongen, R. H. Joho, and A. M. Brown. 1990. Fast and slow gating of sodium channels encoded by a single mRNA. *Neuron*. 4:243–252.
- Nagy, K. 1987. Evidence for multiple open states of sodium channels in neuroblastoma cells. *J. Membr. Biol.* 96:251–262.
- Nagy, K., T. Kiss, and D. Hof. 1983. Single Na channels in mouse neuroblastoma cell membrane. Indications for two open states. *Pflugers Arch. Eur. J. Physiol.* 399:302–308.
- Oxford, G. S., and J. Z. Yeh. 1985. Interactions of monovalent cations with sodium channels in the squid axon. I. Modification of physiological inactivation gating. *J. Gen. Physiol.* 85:583–602.
- Patlak, J. B., and M. Ortiz. 1986. Two modes of gating during late Na⁺ channel currents in frog Sartorius muscle. *J. Gen. Physiol.* 87:305–326.
- Quandt, F., and T. Narahashi. 1982. Modification of single channels by batrachotoxin. *Proc. Natl. Acad. Sci. USA*. 79:6732–6736.
- Rao, R. C. 1973. Linear Statistical Inference and Its Applications. Second Edition. John Wiley & Sons, Inc., New York. 625 pp.
- Roux, B., and R. Sauve. 1985. A general solution to the time interval omission problem applied to single channel analysis. *Biophys. J.* 48:149–158.
- Scanley, B. E., D. A. Hanck, T. Chay, and H. A. Fozzard. 1990. Kinetic analysis of single sodium channels from canine cardiac purkinje cells. *J. Gen. Physiol.* 95:411–437.
- Shoukimas, J. J., and R. J. French. 1980. Incomplete inactivation of sodium currents in nonperfused squid axons. *Biophys. J.* 32:857–862.
- Sigworth, F. 1981. Covariance of nonstationary sodium current fluctuations at the Node of Ranvier. *Biophys. J.* 34:111–133.
- Sigworth, F., and S. M. Sine. 1987. Data transformation for improved display and fitting of single channel dwell time histograms. *Biophys. J.* 52:1047–1054.
- Spiegel, M. R. 1961. Theory and Problems of Statistics. Schaum Publishing Co., New York. 359 pp.
- Stimers, J. R., F. Bezanilla, and R. E. Taylor. 1985. Sodium channel activation in the squid giant axon. Steady state properties. *J. Gen. Physiol.* 85:65–82.
- Stimers, J. R., F. Bezanilla, and R. E. Taylor. 1987. Sodium channel gating currents. Origin of the rising phase. *J. Gen. Physiol.* 89:521–540.
- Tanguy, J., and J. Z. Yeh. 1988. Batrachotoxin uncouples charge immobilization from fast inactivation in squid giant axon. *Biophys. J.* 54: 719–730.
- Vandenberg, C. A., and F. Bezanilla. 1991a. A sodium channel model based on single channel, macroscopic ionic, and gating currents in the squid giant axon. *Biophys. J.* 60:1511–1533.
- Vandenberg, C. A., and F. Bezanilla. 1991b. Single-channel, macroscopic, and gating currents from sodium channels in the squid giant axon. *Biophys. J.* 60:1499–1510.
- Zhou, J., J. F. Potts, J. S. Trimmer, W. S. Agnew, and F. J. Sigworth. 1991. Multiple gating modes and the effect of modulating factors on the μ I sodium channel. *Neuron*. 7:775–785.